Magnetic impurities in spin-split superconductors

W.-V. van Gerven Oei,[1] D. Tanasković,[1] and R. Žitko[2]
[1]*Scientific Computing Laboratory, Center for the Study of Complex Systems, Institute of Physics Belgrade, University of Belgrade, Pregrevica 118, 11080 Belgrade, Serbia*
[2]*Jožef Stefan Institute, Jamova 39, SI-1000 Ljubljana, Slovenia*

(Received 25 November 2016; revised manuscript received 25 January 2017; published 13 February 2017)

Hybrid semiconductor-superconductor quantum dot devices are tunable physical realizations of quantum impurity models for a magnetic impurity in a superconducting host. The binding energy of the localized subgap Shiba states is set by the gate voltages and external magnetic field. In this work we discuss the effects of the Zeeman spin splitting, which is generically present both in the quantum dot and in the (thin-film) superconductor. The unequal g factors in semiconductor and superconductor materials result in respective Zeeman splittings of different magnitude. We consider both classical and quantum impurities. In the first case we analytically study the spectral function and the subgap states. The energy of bound states depends on the spin-splitting of the Bogoliubov quasiparticle bands as a simple rigid shift. For the case of collinear magnetization of impurity and host, the Shiba resonance of a given spin polarization remains unperturbed when it overlaps with the branch of the quasiparticle excitations of the opposite spin polarization. In the quantum case, we employ numerical renormalization group calculations to study the effect of the Zeeman field for different values of the g factors of the impurity and of the superconductor. We find that in general the critical magnetic field for the singlet-doublet transition changes nonmonotonically as a function of the superconducting gap, demonstrating the existence of two different transition mechanisms: Zeeman splitting of Shiba states or gap closure due to Zeeman splitting of Bogoliubov states. We also study how in the presence of spin-orbit coupling, modeled as an additional noncollinear component of the magnetic field at the impurity site, the Shiba resonance overlapping with the quasiparticle continuum of the opposite spin gradually broadens and then merges with the continuum.

DOI: 10.1103/PhysRevB.95.085115

I. INTRODUCTION

The interest in bound states induced by magnetic impurities in superconductors, predicted in the early works of Yu, Shiba, and Rusinov [1–3], has been recently revived by the advances in the synthesis and characterization of semiconductor-superconductor nanostructures [4–9] and in the tunneling spectroscopy of magnetic adsorbates on superconductor surfaces [10–15]. In particular, hybrid devices based on quantum dots can be used as fully controllable physical realizations of quantum impurity models with gapped conduction bands [16–27]. The ground state of the quantum dot can be tuned to be either a spin singlet or a spin doublet depending on the impurity level and the hybridization with the bulk superconductor [5,6,28–31]. The Coulomb interaction on the quantum dot favors the spin doublet ground state, while the spin singlet can be stabilized by the Kondo effect or by pairing due to the superconducting proximity effect [32–36]. The position of the in-gap (Shiba) resonances, as determined from the tunneling conductance, agrees even quantitatively with the calculations based on the simple single-orbital Anderson impurity model [37,38].

Very recently, research has focused on the effects of the magnetic field on the in-gap states [39–48] because systems of this class have been proposed as possible building blocks for topologically ordered systems exhibiting Majorana edge states [49–52]. These are significant for fundamental reasons and might also find application in quantum computation [53–55]. When an external magnetic field is applied to a thin-film superconductor in the parallel (in-plane) direction, the superconducting state persists to relatively large fields. The quasiparticle states become, however, strongly spin polarized and the coherence peaks in the density of states become Zeeman split [56–60]: Systems in this regime are known as spin-split or Zeeman-split superconductors, and play a key role in the emerging field of superconducting spintronics [61]. The spectral function of a spin-split superconductor has two band edges with diverging coherence peaks separated by the bulk Zeeman energy, reflecting the fact that the Bogoliubov excitations have spin-dependent energies $E_{k\sigma}=\sqrt{\xi_k^2+\Delta^2}+g_{\text{bulk}}\mu_B B\sigma$. Here $\xi_k = \epsilon_k - \mu$ is the energy level ϵ_k of electron with momentum k measured with respect to the chemical potential μ, Δ is the gap, g_{bulk} is the g factor of the superconductor, μ_B is the Bohr magneton, B is the magnetic field, and $\sigma = \pm 1/2$ is the quasiparticle spin. Since the Shiba states can be considered as bound states of Bogoliubov quasiparticles, the spectral properties of magnetic impurities in spin-split superconductors are modified.

The theoretical work has, so far, mainly focused on the effect of a local magnetic field applied on the position of the impurity only [45,46]. For bulk electrons in the normal state, this approximation is usually justified because the impurity magnetic susceptibility is typically much larger ($\chi_{\text{imp}} \propto 1/T_K$, where T_K is the Kondo temperature) than that of the bulk electrons (Pauli susceptibility, $\chi_{\text{bulk}} \propto \rho \propto 1/D$, where ρ is the density of states at the Fermi level and D is the bandwidth). In superconductors, however, the Zeeman splitting of the Bogoliubov quasiparticle bands and the Zeeman splitting of the doublet subgap states are of comparable magnitude: The splitting of the first is simply the Zeeman energy $g_{\text{bulk}}\mu_B B$, while the splitting of the second is $\tilde{g}_{\text{imp}}\mu_B B$, where $\tilde{g}_{\text{imp}}$ is the impurity g factor g_{imp} renormalized by the coupling with the bulk. Generically, both splittings are comparable with the possible exception of nanowire quantum dots made of materials with extremely strong spin-orbit (SO) coupling and hence very high bare $g_{\rm imp}$. For this reason, it is important to include the Zeeman terms both in the impurity and in the bulk part of the Hamiltonian.

We introduce the ratio r of the Landé g factors which describe the magnitude of the Zeeman splittings:

$$r = g_{\rm bulk}/g_{\rm imp}. \tag{1}$$

For many elemental superconductors the g factor is close to the free electron value, $g_{\rm bulk} \approx 2$. In semiconductors the g factor usually differs strongly from this value due to SO coupling. The effective g factors are quite variable [62]: They can be very large positive, as well as very large negative, or can even be tuned close to 0. The control of g can be achieved through strain engineering [63], nanostructuring [64], or by electrical tuning in quantum dots [62,65–67]. In the $r = 0$ limit, the Zeeman term is only present on the impurity site: This limit is appropriate for materials with very large positive or negative g factor, where the Zeeman splitting in the superconductor is indeed negligible. Another special limit is $r = 1$, where all sites (bulk and impurity) have the same g factor. In general, however, the value of r is essentially unconstrained.

Here we study, using analytical calculations for a classical impurity (with no internal dynamics) and with the numerical renormalization group (NRG) method [22,68–74] for a quantum impurity (which incorporates the effect of spin flips), the spectral properties of the Shiba states. In the classical case we perform a calculation along the lines of Refs. [1–3], but include the effect of the Zeeman term in the superconductor. In the quantum case we focus on the single-orbital Anderson impurity and discuss the changes in the singlet-doublet phase transition as the ratio of the g factors of the impurity and the bulk is varied. We study the fate of a subgap resonance when it approaches the continuum of the Bogoliubov quasiparticles with the opposite spin, with and without the additional transverse magnetic field that mimics noncollinearity in the presence of SO coupling.

II. CLASSICAL IMPURITY

Initially, the impurity is described using a quantum mechanical spin-S operator, which is exchange coupled with the spin density of the conduction band electrons at the position of the impurity at $\mathbf{r} = 0$. The corresponding Hamiltonian is $H = H_{\rm BCS} + H_{\rm imp}$ with

$$H_{\rm BCS} = \sum_{k\sigma} \xi_k c^\dagger_{\mathbf{k},\sigma} c_{\mathbf{k},\sigma} - \Delta \sum_k (c^\dagger_{\mathbf{k},\uparrow} c^\dagger_{-\mathbf{k},\downarrow} + \text{H.c.}) + \sum_k b_{\rm bulk} s_{z,\mathbf{k}} \tag{2}$$

and

$$H_{\rm imp} = J\mathbf{S} \cdot \mathbf{s}(\mathbf{r} = 0), \tag{3}$$

where $b_{\rm bulk} = g_{\rm bulk}\mu_B B$ is the magnetic field expressed in the energy units (i.e., the Zeeman splitting), $s_{z,\mathbf{k}} = \frac{1}{2}(n_{\uparrow,\mathbf{k}} - n_{\downarrow,\mathbf{k}})$, and $\mathbf{s}(\mathbf{r} = 0) = \frac{1}{N}\sum_{\mathbf{k}} \mathbf{s}_{\mathbf{k}}$. J is the exchange coupling between the impurity and the host. All other quantities have already been defined in the previous section. The classical impurity limit consists of taking the $S \to \infty$ limit while keeping $JS = \text{const}$. In this limit, the longitudinal component of the exchange interaction persists, while the transverse (spin-flip) components decrease as $1/S$ and hence drop out of the problem. The Hamiltonian then becomes noninteracting. We introduce the effective local field

$$h = JS \tag{4}$$

and the dimensionless impurity coupling parameter

$$\alpha = \pi\rho h/2 = \pi\rho JS/2, \tag{5}$$

where ρ is the density of states (DOS) at the Fermi level in the normal state. We will first assume that the bulk field $b_{\rm bulk}$ and the effective local field h are collinear and of the same sign. To be specific, we choose $b_{\rm bulk} > 0$, $h > 0$.

The nonperturbed Green's function of the Zeeman-split superconductor is

$$G^0_k(z) = \frac{(z - b_{\rm bulk}/2)\tau_0 + \epsilon_k\tau_3 - \Delta\tau_1}{(z - b_{\rm bulk}/2)^2 - \left(\epsilon_k^2 + \Delta^2\right)}. \tag{6}$$

Here τ_1,τ_2,τ_3 are the Pauli matrices, τ_0 is the identity matrix, and z is the frequency argument. To obtain the local Green's function at the origin, $G^0_{\rm loc}$, we sum over the momenta k and switch over to an integral over energies assuming a flat DOS in the normal state. In the wide-band limit we find

$$G^0(z) = -\pi\rho\frac{(z - b_{\rm bulk}/2)\tau_0 - \Delta\tau_1}{\sqrt{\Delta^2 - (z - b_{\rm bulk}/2)^2}}. \tag{7}$$

The Dyson's equation to include the impurity effect can be written as [1–3]

$$[G(z)]^{-1} = [G^0(z)]^{-1} - h\tau_0. \tag{8}$$

We have

$$[G^0(z)]^{-1} = -\frac{\sqrt{\Delta^2 - \left(z - \frac{b_{\rm bulk}}{2}\right)^2}}{\pi\rho\left[\left(z - \frac{b_{\rm bulk}}{2}\right)^2 - \Delta^2\right]}[(z - b_{\rm bulk}/2)\tau_0 + \Delta\tau_1], \tag{9}$$

and finally

$$G(z) = -\pi\rho\frac{1}{D}\begin{pmatrix} a & \Delta \\ \Delta & a \end{pmatrix}, \tag{10}$$

where

$$D = 2\alpha\left(\frac{b_{\rm bulk}}{2} - z\right) + (\alpha^2 - 1)\sqrt{\Delta^2 - \left(\frac{b_{\rm bulk}}{2} - z\right)^2},$$
$$a = b_{\rm bulk}/2 - z + \alpha\sqrt{\Delta^2 - (b_{\rm bulk}/2 - z)^2}. \tag{11}$$

The spin-up spectral function is $A_\uparrow(\omega) = -(1/\pi)\text{Im}G_{11}(\omega + i\delta)$, while the spin-down spectral function is $A_\downarrow(\omega) = -(1/\pi)\text{Im}[-G_{22}(-\omega - i\delta)] = -(1/\pi)\text{Im}G_{22}(-\omega + i\delta)$.

The 11 (spin-up) matrix component of $G(z)$ has two poles:

$$\omega_{1,2} = b_{\rm bulk}/2 \pm \Delta\frac{1 - \alpha^2}{1 + \alpha^2}. \tag{12}$$

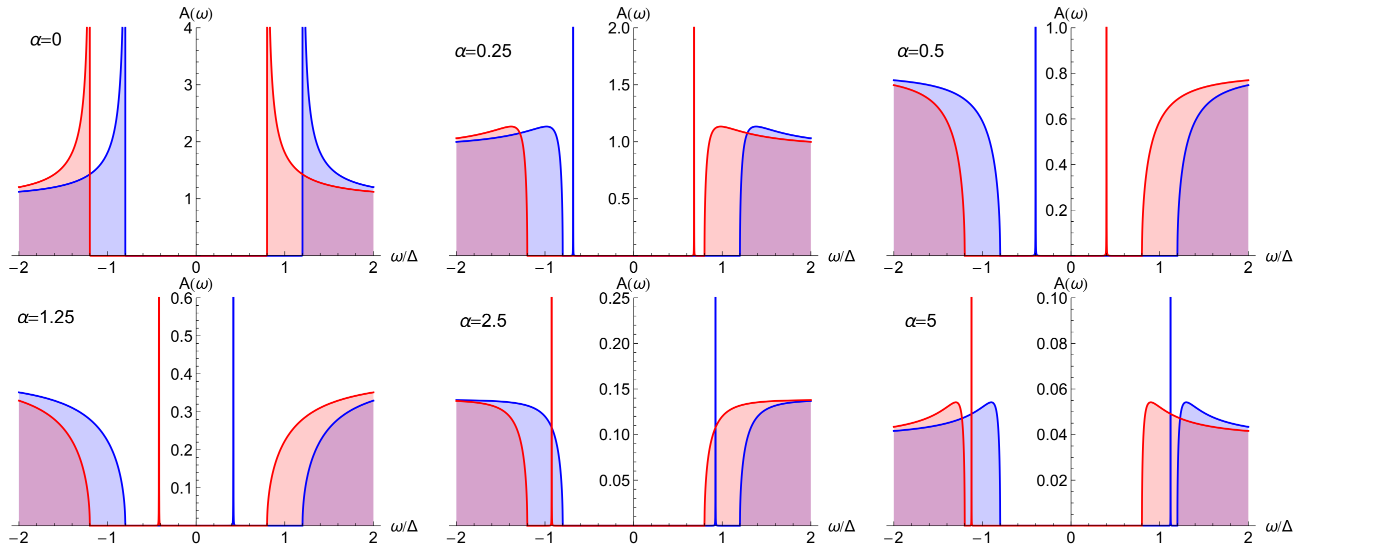

FIG. 1. Spin-projected spectral functions (blue for spin-up, red for spin-down) for a range of the dimensionless impurity coupling $\alpha = \pi\rho JS/2$ in a Zeeman-split superconductor with $b_{\text{bulk}}/\Delta = 0.4$.

Only one pole has a finite residue. For $h > 0$ (hence $\alpha > 0$) we find a subgap resonance in the spin-up spectral function at

$$\omega_\uparrow = b_{\text{bulk}}/2 - \Delta\frac{1-\alpha^2}{1+\alpha^2}. \tag{13}$$

Conversely, the spin-down spectral function has a resonance at $\omega_\downarrow = -\omega_\uparrow$:

$$\omega_\downarrow = -b_{\text{bulk}}/2 + \Delta\frac{1-\alpha^2}{1+\alpha^2}. \tag{14}$$

We emphasize that the spin-projected spectral functions have a single subgap resonance, one for each spin. This is to be contrasted with the behavior of the quantum model discussed in the following section which has (in the spin-singlet regime for finite magnetic field) two resonances in each spin-projected spectral function. This is a clear indication of the different degeneracies of states in the classical and quantum impurity models.

Some representative spectra are plotted in Fig. 1. The $\alpha = 0$ case corresponds to the limit of a clean Zeeman-split superconductor. Each quasiparticle continuum branch has a characteristic inverse square root divergence at its edge.

For small $\alpha = 0.25$, the Shiba bound states emerge out of the quasiparticle continuum, the spin-up resonance in the negative part of the spectrum, and the spin-down resonance in the positive part, in line with Eqs. (13) and (14) for small α. The shift by $b_{\text{bulk}}/2$ is expected, since the spin-up Shiba state is generated by the Bogoliubov states with spin up, which are themselves shifted by the same amount. Conversely, the spin-down Shiba state is generated as a linear superposition of Bogoliubov states with spin down, which are shifted by $-b_{\text{bulk}}/2$. We observe that *all four* branches of the quasiparticle band lose their inverse square-root singularity and contribute spectral weight to the nascent Shiba state (see also Ref. [48]), not only the "inner" ones (spin-up occupied and spin-down unoccupied).

With increasing α, the Shiba states move toward the gap center (chemical potential) and they cross when the condition

$$b_{\text{bulk}}/2 = \Delta\frac{1-\alpha^2}{1+\alpha^2} \tag{15}$$

is met, i.e., at

$$\alpha^* = \frac{\sqrt{1-b_{\text{bulk}}/2\Delta}}{\sqrt{1+b_{\text{bulk}}/2\Delta}}. \tag{16}$$

For $b_{\text{bulk}}/\Delta = 0.4$, as used here, this happens at $\alpha^* \approx 0.82 < 1$. This signals the occurrence of the quantum phase transition in which the fermion parity of the (sub)system changes. We also note that alternatively, for constant $\alpha < 1$, the transition can be driven by the external magnetic field.

For still larger $\alpha = 2.5$, the spin-up Shiba resonance overlaps with the spin-down quasiparticle continuum (and vice versa for the spin-down Shiba resonance), but since the spin is assumed to be a good quantum number there is no broadening of the Shiba resonances. (See below, Sec. III B, for a discussion of the SO effects in the case of a quantum impurity.)

For very large values of α, the Shiba states eventually merge with the continuum again. This trend is accompanied by the reappearance of the inverse square-root resonances, an indication of which is visible for $\alpha = 5$ in Fig. 1.

We now discuss the case of antialigned fields, taking $b_{\text{bulk}} > 0$ and $h < 0$. In this case, for small $|\alpha|$ the spin-up Shiba state occurs at

$$\omega_\uparrow = b_{\text{bulk}}/2 + \Delta\frac{1-\alpha^2}{1+\alpha^2}, \tag{17}$$

and hence overlaps with the continuum of spin-down quasiparticles for $|\alpha| < 1/\sqrt{2\Delta/b_{\text{bulk}} - 1}$. The quantum phase transition occurs for

$$|\alpha^*| = \frac{\sqrt{1+b_{\text{bulk}}/2\Delta}}{1-b_{\text{bulk}}/2\Delta} > 1. \tag{18}$$

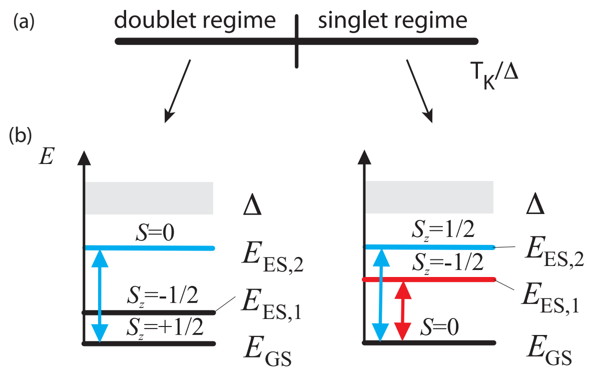

FIG. 2. (a) Schematic phase diagram for $B=0$. (b) Subgap splitting for finite field B.

For large $|\alpha|$ the Shiba states again merge with the continuum at the inner edges of the Bogoliubov bands. The regimes that the system goes through for $\alpha<0$ are thus in the opposite order to those for $\alpha>0$.

The main deficiency of the impurity model in the classical limit is the reduced multiplicity of the subgap states. Physically, this is due to the fact that in the classical limit the effective impurity potential for particle-like excitations is attractive for one spin orientation and repulsive for the other; hence a single bound state is generated for a given spin orientation. The spin-flip processes in the quantum model lead to a situation where the effective potential is attractive for both spin polarizations, hence twice the degeneracy. We discuss this more general situation in the following section.

III. QUANTUM IMPURITY

A. Model and method

We consider a single spin-$\frac{1}{2}$ impurity level with on-site Coulomb interaction. The Hamiltonian is given by

$$
\begin{aligned}
H = &\sum_{\mathbf{k},\sigma} \epsilon_{\mathbf{k}} c^\dagger_{\mathbf{k}\sigma} c_{\mathbf{k}\sigma} - \Delta \sum_{\mathbf{k}} (c^\dagger_{\mathbf{k}\uparrow} c^\dagger_{-\mathbf{k}\downarrow} + \text{H.c.}) \\
&+ V \sum_{\mathbf{k},\sigma} (d^\dagger_\sigma c_{\mathbf{k}\sigma} + \text{H.c.}) + \epsilon_d \sum_\sigma n_\sigma + U n_\uparrow n_\downarrow \\
&+ g_{\text{imp}} \mu_B (B S_z + B_x S_x) + g_{\text{bulk}} \mu_B B \sum_{\mathbf{k}} s_{z,\mathbf{k}}. \qquad (19)
\end{aligned}
$$

$d^\dagger_\sigma$ is the creation operator on the impurity which is hybridized with the bulk by V and has the energy level ϵ_d. $n_\sigma = d^\dagger_\sigma d_\sigma$, $S_z = \frac{1}{2}(d^\dagger_\uparrow d_\uparrow - d^\dagger_\downarrow d_\downarrow)$, $S_x = \frac{1}{2}(d^\dagger_\uparrow d_\downarrow + d^\dagger_\downarrow d_\uparrow)$, $s_{z,\mathbf{k}} = \frac{1}{2}(c^\dagger_{\mathbf{k}\uparrow} c_{\mathbf{k}\uparrow} - c^\dagger_{\mathbf{k}\downarrow} c_{\mathbf{k}\downarrow})$. The magnetic field B couples with the quantum dot by the g factor equal to g_{imp} and with the superconductor by g_{bulk}. The transverse magnetic field which can flip the spin is introduced through the parameter B_x. We will consider a flat particle-hole symmetric band of half-width D so that $\rho = 1/2D$. The hybridization strength is characterized by $\Gamma = \pi\rho V^2$.

We employ the NRG method to solve the problem. There are two ways to introduce a bulk Zeeman field in the NRG: as local Zeeman terms on all sites of the Wilson chain, or through a separate discretization of spin-up and spin-down densities of states shifted by the Zeeman term [75]. The former approach is suitable for models with a spectral gap, as discussed here, while the latter has to be used for spin-polarized metals with finite DOS at the Fermi level. We use a fine discretization mesh with twist averaging over $N_z = 64$ grids so that high spectral

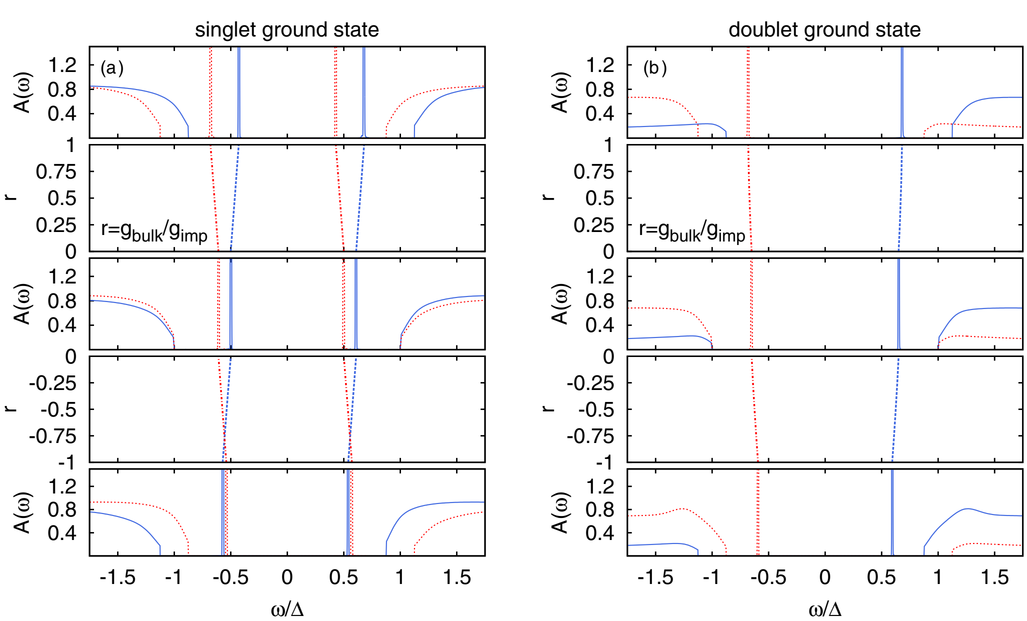

FIG. 3. Spectral function of the impurity for the spin singlet (a) and spin doublet ground state (b). The parameters are $b_{\text{imp}}/U = 0.005$ and $\Delta/U = 0.02$. For the singlet ground state $\Gamma/U = 0.2$ and for the doublet $\Gamma/U = 0.075$. The spectrum for $r = g_{\text{bulk}}/g_{\text{imp}} = 0$ is shown in central panels, the adjoining panels show the evolution of the position of the Shiba resonances as $|r|$ increases, and the top/bottom panels correspond to $r=1$ and $r=-1$, respectively.

resolution is possible inside the gap and in the vicinity of the gap edges, which are the regions of main interest in this work. The only conserved quantum number in the presence of an external field along the z axis is the projection of total spin S_z, i.e., the problem has U(1) spin symmetry. Other parameters are $\Lambda = 2$, the NRG truncation cutoff energy is $10\epsilon_N$ where $\epsilon_N \propto \Lambda^{-N/2}$ is the energy scale at the Nth step of the iteration, and at least 200 states were used at late iterations N when the gap is opened. The spectral functions are computed with the DMNRG algorithm [70] with the $N/N+2$ scheme for patching the spectral functions. This approach allows maximal spectral resolution at zero temperature. The broadening is performed on a logarithmic mesh with a small ratio $r = 1.01$ between two energies outside the gap and on a linear mesh inside the gap. As can be seen in the figures further down, the use of these different broadening kernels leads to some artifacts at the continuum edges. All calculations are performed in the zero-temperature limit, $T = 0$.

Unless otherwise specified, the model parameters are $U/D = 1$, $\Delta/U = 0.02$, and $\epsilon_d = -U/2$.

The ground state of the Anderson impurity model, Eq. (19), in the absence of the magnetic field is either a singlet or a doublet depending on the ratio of the Kondo temperature [68,69] $T_K \approx 0.18U\sqrt{8\Gamma/\pi U}\exp(-\pi U/8\Gamma)$ and the superconducting gap Δ. The impurity spin is screened by the conduction electrons for $\Delta < \Delta_c$ forming a spin singlet, while for $\Delta > \Delta_c$ the local moment is unscreened and the ground state forms a spin doublet; here $\Delta_c \approx T_K/0.3$ [17,18,22] in the limit $U/\Gamma \ll 1$. At the quantum phase transition the energy of the excited many-particle state goes to zero, and the energy levels cross. The transition is accompanied by a jump in the spectral weight of the in-gap resonances and a change of sign of the pairing amplitude [34]. The Zeeman field B lifts the degeneracy of the doublet state [44–46,76]. For a spin singlet ground state, the in-gap resonances corresponding to the doublet state are split in the magnetic field B. In the case of doublet ground state, the positions of the singlet Shiba resonances are shifted in the Zeeman field.

Figure 2 shows a schematic phase diagram in zero magnetic field and the evolution of the energy levels of the ground and excited states with increasing Zeeman magnetic field. This evolution of the in-gap resonances with changes of the hybridization and the magnetic field has been recently observed in tunneling experiments and agrees with the theoretical predictions in the case when the field is coupled only with impurity [44–47]. Here, we explore the fate of the subgap states when the magnetic field is also Zeeman coupled with the bulk superconductor.

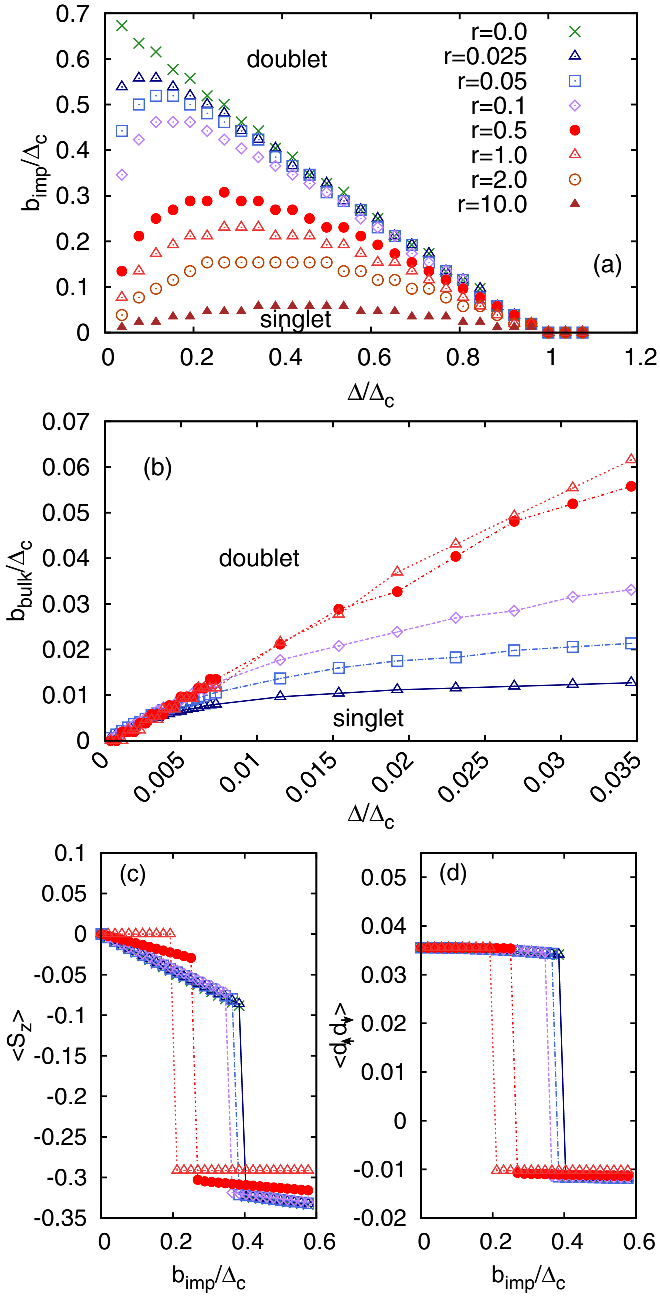

FIG. 4. (a) Phase diagram in the (B,Δ) plane for several values of $r = g_{\rm bulk}/g_{\rm imp}$. Here $\Gamma/U = 0.2$, $\Delta_c/U \approx 0.13$. (b) For small Δ the singlet-doublet transition coincides with the closure of the SC gap for $b_{\rm bulk} \approx 2\Delta$. (c) The expectation value $\langle S_z\rangle$ and (d) the pairing amplitude $\langle d_\uparrow d_\downarrow\rangle$ abruptly change across the phase transition. Here $\Delta = 0.385\Delta_c$.

B. Results

We now discuss the spectral function of the impurity in different parameter regimes and identify the boundary of the singlet-doublet phase transition in the (B,Δ) parameter plane for different values of the g-factor ratio r.

We first consider the case of singlet ground state. In the magnetic field the subgap resonance (which is a spin doublet) splits to its spin-up and spin-down components. The impurity spectral function for $\Gamma/U = 0.2$, $b_{\rm imp}/U = 0.005$ is shown in Fig. 3(a) for $r = 0$ (central panel), $r = 1$ (top panel), and $r = -1$ (bottom panel). The additional panels show how the position of the resonances shifts as the parameter r is varied. For $r = 1$ the expectation value of the spin projection $\langle S_z\rangle$ at the impurity site is $\langle S_z\rangle = 0$ [see Fig. 4(c) and the appendix]. Such compensation holds also in the particle-hole asymmetric case as long as $g_{\rm imp} = g_{\rm bulk}$. If the g factors are different, there will be net magnetization at the impurity site even if the ground state is a spin singlet and there is a finite gap to excited states.

We next consider the case of smaller hybridization, $\Gamma/U = 0.075$, so that the impurity is in the doublet ground state. The spectral functions for $r = 0$, $r = 1$, and $r = -1$, as well as the evolution between them, are shown in Fig. 3(b). A single resonance is now visible for $\omega > 0$, since the ground state has spin projection $S_z = 1/2$, and the only possible excitation is adding a spin-up particle to form a $S_z = 0$ singlet state. We also observe notable differences in the appearance of the gap edges for both spin projections, related to the strong spin polarization of the impurity state in the doublet regime. We emphasize that this distinguishing feature is not present in the classical impurity model discussed above.

The phase diagram in the (B,Δ) plane is shown in Fig. 4. This plot represents the main result of this work. In the absence of a magnetic field, the ground state changes from singlet to doublet for $\Delta = \Delta_c = 0.13U$. Here, $T_K \approx 0.018U$ and $T_K/\Delta_c = 0.138$ for the chosen value of $\Gamma/U = 0.2$. For $\Delta < \Delta_c$ the transition can be also induced by changing the magnetic field. For $r = 0$ the magnetic field is coupled only with the impurity. In this case, as shown in Ref. [45], the critical magnetic field B_c for the singlet-doublet transition linearly depends on the gap, $B_c \sim \Delta_c - \Delta$. For $r \neq 0$, however, B_c has nonmonotonic dependence on Δ: It increases approximately linearly with Δ as it gets reduced from Δ_c, reaches a maximum, and then decreases to zero as $\Delta \to 0$. For $\Delta \sim \Delta_c$ the singlet-doublet transition is a consequence of a competition of three characteristic energies: Δ, T_K, and B. For very small values of Δ (for $\Delta \ll \Delta_c$) the singlet-doublet transition coincides with the closure of the superconducting gap for $b_{\text{bulk}} = 2\Delta$. The phase boundary for small value of Δ is shown in Fig. 4(b). We note that for small Δ the transition to the normal phase would actually occur for smaller value of B, $B = B_{\text{cl}} = \sqrt{g}\Delta \approx \sqrt{2}\Delta$, known as the Clogston limit [77,78]. For $B > B_{\text{cl}}$ the normal phase has lower free energy than the superconducting one. Our main focus is, however, on larger values of the superconducting gap when it is comparable to the Kondo temperature.

The average value of the projection of the local spin $\langle S_z\rangle$ abruptly changes at the phase transition, Fig. 4(c). For $g_{\text{imp}} = g_{\text{bulk}}$, i.e., for $r = 1$, the average value $\langle S_z\rangle = 0$ in the singlet case (see also the appendix). For $r \neq 1$, $\langle S_z\rangle$ is nonzero but small for singlet ground state, and it jumps to large absolute value by increasing the magnetic field at the transition to doublet ground state. The pairing amplitude on the impurity, $\langle d_\uparrow d_\downarrow\rangle$, shows a characteristic sign change at the transition, Fig. 4(d).

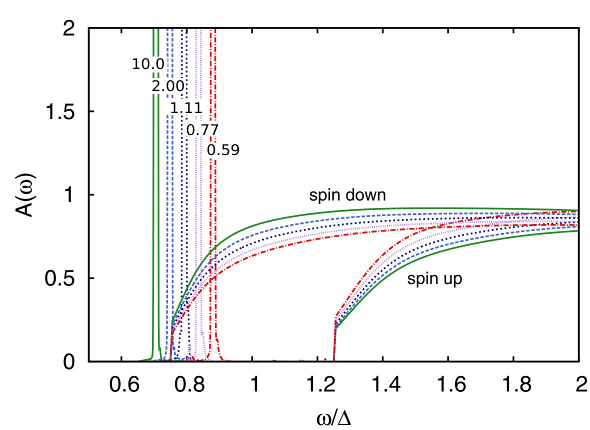

FIG. 5. Spin up in-gap resonances and continuum of excitations for several values of r. Here $b_{\text{bulk}}/U = 0.01$ was kept constant. The finite width of the Shiba resonances is a broadening artifact: These resonances are true δ peaks at zero temperature.

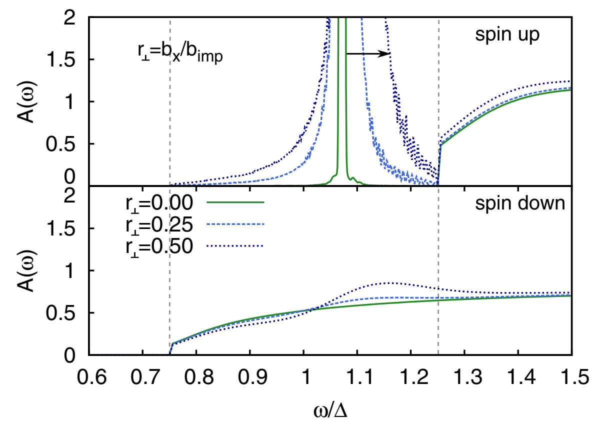

FIG. 6. Spectral function of the spin-up Shiba resonance and the quasiparticle continuum for several values of the spin-flipping transverse magnetic field. As b_x increases, the Shiba resonance broadens.

When the spin-up Shiba state begins to overlap with the spin-down branch of Bogoliubov excitations, it remains unperturbed, as in the classical impurity model. This is the case in spite of the spin-flip processes in the quantum model and is a simple consequence of the conservation of the spin projection S_z quantum number. In other words, the spin-up Shiba state is a bound state of spin-up Bogoliubov quasiparticles, which are orthogonal to and do not mix with the spin-down Bogoliubov quasiparticles. This is illustrated in Fig. 5. Here g_{bulk} and B were kept constant, while the position of the spin-up resonance was changed by changing g_{imp}. A transverse magnetic field, however, flips the spin and the Shiba resonances broaden, as illustrated in Fig. 6. Such broadening effects are expected in realistic systems due to SO coupling.

IV. CONCLUSION

We have analyzed the behavior of magnetic impurities coupled to superconductors subject to an applied magnetic field that does not fully suppress the superconducting order but strongly spin splits the Bogoliubov quasiparticle continua because of the Zeeman coupling. This situation commonly occurs when the field is applied in the plane of a superconducting thin layer and leads to clearly observable effects.

For a classical impurity, approximated as a static local pointlike magnetic field (and aligned with the external field), we find that the position of the Shiba state is shifted linearly with the external field as a simple consequence of the shifting edges of the quasiparticle bands. In fact, the only effect of the spin splitting of the Bogoliubov states is that the frequency argument in the impurity Green's function is shifted as $\omega \to \omega + b_{\text{bulk}}/2$ for spin-up and $\omega \to \omega - b_{\text{bulk}}/2$ for spin-down particles. The parity-changing quantum phase transition no longer occurs at $\alpha = \pi\rho J S/2 = 1$, but rather when the condition $b_{\text{bulk}} = g_{\text{bulk}}\mu_B B/2 = \Delta(1-\alpha^2)/(1+\alpha^2)$ is met. This occurs for $\alpha = \alpha^* < 1$. We observed that for large α the Shiba state of a given spin may overlap with the quasiparticle continuum of the opposite spin and still remain a sharp resonance (a δ peak). This remains true as long as there is no matrix element linking the quasiparticles of both spins.

We then turned to the case of a quantum impurity with far more complex behavior. The Zeeman coupling is present both in the bulk and on the impurity site, and generically the corresponding g factors are different: This is typically indeed the case in the nanoscale hybrid superconductor-semiconductor devices. We find a very significant effect of the Zeeman splitting of the quasiparticle continua: The phase diagram of the possible many-particle ground states (singlet or doublet) in the (Δ,B) plane actually has two very different regimes. In the $\Delta \to \Delta_c$ limiting regime, the transition occurs because a strong enough field decreases the energy of spin-down doublet state below that of the singlet state. In this regime, the phase boundary in the (Δ,B) plane has a negative slope: The closer Δ is to Δ_c, the smaller the separation between the singlet and doublet states in the absence of the field and hence a smaller Zeeman splitting is necessary to induce the transition. We have established that for finite $r = g_{\text{bulk}}/g_{\text{imp}}$ the splitting between the doublet subgap states is larger than for $r = 0$ and hence the separation between the singlet and the spin-down doublet is smaller; thus the transition occurs for a smaller value of the magnetic field. In the other limiting regime of small Δ, the transition occurs because the gap between the spin-polarized Bogoliubov bands closes and the transition line is given asymptotically as $b_{\text{bulk}}/2 = \Delta$; hence the transition line has a positive slope. In reality, such transition is of course preempted by a bulk transition to the normal state (Clogston limit). Nevertheless, even in the physically accessible regime we observe that the actual behavior is determined by a competition of both trends and that the slope of the transition line changes at some intermediate point where the system crosses over from one limiting behavior to another. The actual transition line is therefore bell-shaped and depends on the value of r. The straight line found in the limit $r \to 0$ is, in fact, highly anomalous, and for realistic values of the ratio r there will be a significant degree of curvature.

We have confirmed the possibility of a sharp Shiba resonance overlapping with the continuum of opposite-spin Bogoliubov quasiparticles. In addition, we have considered the gradual widening of the Shiba resonance if local spin-flip processes are allowed (generated, e.g., by SO coupling leading to noncollinear effective magnetic fields): Such processes lead to the hybridization of the Shiba state and its gradual engulfing in the continuum.

In conclusion, we have established the importance of including the Zeeman splitting in the bulk of the superconductor when discussing the effect of the external magnetic field on the subgap states induced by magnetic impurities in superconductors.

ACKNOWLEDGMENTS

W.V.v.G. and D.T. were supported by the Serbian Ministry of Education, Science and Technological Development under Project ON171017 and by the European Commission under H2020 project VI-SEEM, Grant No. 675121. R.Ž. acknowledges the support of the Slovenian Research Agency (ARRS) under Programs P1-0044 and J1-7259. The authors acknowledge support from the bilateral Slovenian-Serbian project "Strong electronic correlations and superconductivity."

APPENDIX: NONINTERACTING MODEL

For completeness, in this appendix we define the analytical expression for the noninteracting Anderson impurity model ($U = 0$); see also Ref. [79]. We work in the Nambu space, $D^\dagger = (d^\dagger_\uparrow, d_\downarrow)$, $C^\dagger_k = (c^\dagger_{k\uparrow}, c_{-k\downarrow})$. The Hamiltonian can be written as

$$H_{SC} = \sum_k C^\dagger_k A_k C_k, \tag{A1}$$

where

$$A_k = \begin{pmatrix} \epsilon_k + b_{\text{bulk}}/2 & -\Delta \\ -\Delta & -\epsilon_k + b_{\text{bulk}}/2 \end{pmatrix}. \tag{A2}$$

The Green's function is given by $g_k(z) = (z - A_k)^{-1}$,

$$g_k(z)^{-1} = (z - b_{\text{bulk}}/2)\sigma_0 - \epsilon_k\sigma_3 + \Delta\sigma_1, \tag{A3}$$

with $\sigma_{1,2,3}$ being Pauli matrices and σ_0 being the identity matrix, so that

$$g_k(z) = \frac{(z - b_{\text{bulk}}/2)\sigma_0 + \epsilon_k\sigma_3 - \Delta\sigma_1}{(z - b_{\text{bulk}}/2)^2 - \left(\epsilon_k^2 + \Delta^2\right)}. \tag{A4}$$

The impurity Green's function is

$$G(z)^{-1}(z) = z\sigma_0 - \epsilon_d\sigma_3 - (b_{\text{imp}}/2)\sigma_0 - V^2\sigma_3 \frac{1}{N}\sum_k g_k(z)\sigma_3. \tag{A5}$$

In the wide-band limit

$$-V^2\frac{1}{N}\sigma_3\sum_k g_k(z)\sigma_3 = \Gamma\frac{(z - b_{\text{bulk}}/2)\sigma_0 + \Delta\sigma_1}{E(z - b_{\text{bulk}}/2)}, \tag{A6}$$

where $\Gamma = \pi\rho_0 V^2$. $T \to 0$, on real axis, $z = x + i\delta$:

$$\begin{aligned} E(x) &= -i\,\text{sgn}(x)\sqrt{x^2 - \Delta^2}, \quad \text{for } |x| > \Delta, \\ E(x) &= \sqrt{\Delta^2 - x^2}, \quad \text{for } |x| < \Delta. \end{aligned} \tag{A7}$$

Finally, we have

$$\begin{aligned} G^{-1}(\omega) &= (\omega - b_{\text{imp}}/2)\sigma_0 - \epsilon_d\sigma_3 \\ &\quad + \Gamma\frac{(\omega - b_{\text{bulk}}/2)\sigma_0 + \Delta\sigma_1}{E(\omega - b_{\text{bulk}}/2)}. \end{aligned} \tag{A8}$$

Matrix inversion yields

$$\begin{aligned} G(\omega) = \frac{1}{D(\omega)}\bigg\{ &(\omega - b_{\text{imp}}/2)\left[1 + \frac{\Gamma}{E(\omega - b_{\text{bulk}}/2)}\right]\sigma_0 \\ &- \frac{\Gamma\Delta}{E(\omega - b_{\text{bulk}}/2)}\sigma_1 + \epsilon_d\sigma_3\bigg\}, \end{aligned} \tag{A9}$$

with

$$D(\omega) = (\omega - b_{\rm imp}/2)^2\left[1 + \frac{\Gamma}{E(\omega - b_{\rm bulk}/2)}\right]^2 - \frac{\Gamma^2\Delta^2}{E(\omega - b_{\rm bulk}/2)^2} - \epsilon_d^2. \tag{A10}$$

Now assume $b \equiv b_{\rm imp} = b_{\rm bulk}$. We consider two functions $G_\uparrow(\omega) = G_{11}(\omega + b/2)$ and $G_\downarrow(\omega) = -G_{22}(-\omega - b/2)^*$. Taking into account the symmetry properties of $E(x)$, it is easily shown that $G_\uparrow = G_\downarrow$ both inside and outside the gap. This shows that as long as the system is in the singlet ground state, it is possible to shift the spectral functions of spin-up and spin-down subsystems to make them overlap; thus their integrals over the negative energies (occupied states) are equal and hence $\langle S_z\rangle = 0$. This is also the case in the interacting case. For $b_{\rm imp} \neq b_{\rm bulk}$, $\langle S_z\rangle$ in the singlet regime will be nonzero but small. In the doublet regime, irrespective of the value of $r = b_{\rm bulk}/b_{\rm imp}$, $\langle S_z\rangle$ is large.

[1] L. Yu, Bound state in superconductors with paramagnetic impurities, Acta Phys. Sin. **21**, 75 (1965).

[2] H. Shiba, Classical spins in superconductors, Prog. Theor. Phys. **40**, 435 (1968).

[3] A. I. Rusinov, Superconductivity near a paramagnetic impurity, Zh. Eksp. Teor. Fiz. Pisma Red. **9**, 146 (1968) [JETP Lett. **9**, 85 (1969)].

[4] M. F. Goffman, R. Cron, A. Levy Yeyati, P. Joyez, M. H. Devoret, D. Esteve, and C. Urbina, Supercurrent in Atomic Point Contacts and Andreev States, Phys. Rev. Lett. **85**, 170 (2000).

[5] J.-D. Pillet, C. H. L. Quay, P. Morin, C. Bena, A. Levy Yeyati, and P. Joyez, Andreev bound states in supercurrent-carrying carbon nanotubes revealed, Nat. Phys. **6**, 965 (2010).

[6] R. S. Deacon, Y. Tanaka, A. Oiwa, R. Sakano, K. Yoshida, K. Shibata, K. Hirakawa, and S. Tarucha, Interplay of Kondo and Superconducting Correlations in the Nonequilibrium Andreev Transport Through a Quantum Dot, Phys. Rev. Lett. **104**, 076805 (2010).

[7] S. De Franceschi, L. Kouwenhoven, C. Schönenberger, and W. Wernsdorfer, Hybrid superconductor-quantum dot devices, Nat. Nanotechnol. **5**, 703 (2010).

[8] L. Bretheau, C. O. Girit, C. Urbina, D. Esteve, and H. Pothier, Supercurrent Spectroscopy of Andreev States, Phys. Rev. X **3**, 041034 (2013).

[9] C. Janvier, L. Tosi, L. Bretheau, C. O. Girit, M. Stern, P. Bertet, P. Joyez, D. Vion, D. Esteve, M. F. Goffman, H. Pothier, and C. Urbina, Coherent manipulation of Andreev states in superconducting atomic contacts, Science **349**, 1199 (2015).

[10] A. Yazdani, B. A. Jones, C. P. Lutz, M. F. Crommie, and D. M. Eigler, Probing the local effects of magnetic impurities on superconductivity, Science **275**, 1767 (1997).

[11] S. H. Ji, T. Zhang, Y. S. Fu, X. Chen, X.-C. Ma, J. Li, W.-H. Duan, J.-F. Jia, and Q.-K. Xue, High-Resolution Scanning Tunneling Spectroscopy of Magnetic Impurity Induced Bound States in the Superconducting Gap of Pb Thin Films, Phys. Rev. Lett. **100**, 226801 (2008).

[12] K. J. Franke, G. Schulze, and J. I. Pascual, Competition of superconductivity phenomena and Kondo screening at the nanoscale, Science **332**, 940 (2011).

[13] M. Ruby, F. Pientka, Y. Peng, F. von Oppen, B. W. Heinrich, and K. J. Franke, Tunneling Processes into Localized Subgap States in Superconductors, Phys. Rev. Lett. **115**, 087001 (2015).

[14] M. T. Randeria, B. E. Feldman, I. K. Drozdov, and A. Yazdani, Scanning Josephson spectroscopy on the atomic scale, Phys. Rev. B **93**, 161115 (2016).

[15] N. Hatter, B. W. Heinrich, M. Ruby, J. I. Pascual, and K. J. Franke, Magnetic anisotropy in Shiba bound states across a quantum phase transition, Nat. Commun. **6**, 8988 (2015).

[16] A. Sakurai, Comments on superconductors with magnetic impurities, Prog. Theor. Phys. **44**, 1472 (1970).

[17] K. Satori, H. Shiba, O. Sakai, and Y. Shimizu, Numerical renormalization group study of magnetic impurities in superconductors, J. Phys. Soc. Jpn. **61**, 3239 (1992).

[18] O. Sakai, Y. Shimizu, H. Shiba, and K. Satori, Numerical renormalization group study of magnetic impurities in supercoductors, II: Dynamical excitations spectra and spatial variation of the order parameter, J. Phys. Soc. Jpn. **62**, 3181 (1993).

[19] M. I. Salkola, A. V. Balatsky, and J. R. Schrieffer, Spectral properties of quasiparticle excitations induced by magnetic moments in superconductors, Phys. Rev. B **55**, 12648 (1997).

[20] M. E. Flatté and J. M. Byers, Local Electronic Structure of a Single Magnetic Impurity in a Superconductor, Phys. Rev. Lett. **78**, 3761 (1997).

[21] M. E. Flatté and J. M. Byers, Local electronic structure of defects in superconductors, Phys. Rev. B **56**, 11213 (1997).

[22] T. Yoshioka and Y. Ohashi, Numerical renormalization group studies on single impurity Anderson model in superconductivity: A unified treatment of magnetic, nonmagnetic impurities, and resonance scattering, J. Phys. Soc. Jpn. **69**, 1812 (2000).

[23] D. K. Morr and N. A. Stavropoulos, Quantum interference between impurities: Creating novel many-body states in s-wave superconductors, Phys. Rev. B **67**, 020502(R) (2003).

[24] A. V. Balatsky, I. Vekhter, and J.-X. Zhu, Impurity-induced states in conventional and unconventional superconductors, Rev. Mod. Phys. **78**, 373 (2006).

[25] J. Bauer, A. Oguri, and A. C. Hewson, Spectral properties of locally correlated electrons in a Bardeen-Cooper-Schrieffer superconductor, J. Phys.: Condens. Matter **19**, 486211 (2007).

[26] A. Martín-Rodero and A. Levy Yeyati, Josephson and Andreev transport through quantum dots, Adv. Phys. **60**, 899 (2011).

[27] T. Dirks, T. L. Hughes, S. Lal, B. Uchoa, Y.-F. Chen, C. Chialvo, P. M. Goldbart, and N. Mason, Transport through Andreev bound states in a graphene quantum dot, Nat. Phys. **7**, 386 (2011).

[28] M. R. Buitelaar, T. Nussbaumer, and C. Schonenberger, Quantum Dot in the Kondo Regime Coupled to Superconductors, Phys. Rev. Lett. **89**, 256801 (2002).

[29] R. Maurand, T. Meng, E. Bonet, S. Florens, L. Marty, and W. Wernsdorfer, First-Order 0-π Quantum Phase Transition in the Kondo Regime of a Superconducting Carbon-Nanotube Quantum Dot, Phys. Rev. X **2**, 011009 (2012).

[30] A. Martín-Rodero and A. L. Yeyati, The Andreev states of a superconducting quantum dot: Mean field versus exact numerical results, J. Phys.: Condens. Matter **24**, 385303 (2012).
[31] M. Jarrell, D. S. Sivia, and B. Patton, Gap states in dilute-magnetic-alloy superconductors: A quantum Monte Carlo study, Phys. Rev. B **42**, 4804 (1990).
[32] E. Vecino, A. Martín-Rodero, and A. Yeyati, Josephson current through a correlated quantum level: Andreev states and π junction behavior, Phys. Rev. B **68**, 035105 (2003).
[33] A. Oguri, Y. Tanaka, and A. C. Hewson, Quantum phase transition in a minimal model for the Kondo effect in a Josephson junction, J. Phys. Soc. Jpn. **73**, 2494 (2004).
[34] M.-S. Choi, M. Lee, K. Kang, and W. Belzig, Kondo effect and Josephson current through a quantum dot between two superconductors, Phys. Rev. B **70**, 020502 (2004).
[35] C. Karrasch, A. Oguri, and V. Meden, Josephson current through a single Anderson impurity coupled to BCS leads, Phys. Rev. B **77**, 024517 (2008).
[36] T. Meng, S. Florens, and P. Simon, Self-consistent description of Andreev bound states in Josephson quantum dot devices, Phys. Rev. B **79**, 224521 (2009).
[37] J.-D. Pillet, P. Joyez, R. Žitko, and M. F. Goffman, Tunneling spectroscopy of a single quantum dot coupled to a superconductor: From Kondo ridge to Andreev bound states, Phys. Rev. B **88**, 045101 (2013).
[38] E. J. H. Lee, X. Jiang, R. Žitko, C. M. Lieber, and S. De Franceschi, Scaling of sub-gap excitations in a superconductor-semiconductor nanowire quantum dot, arXiv:1609.07582.
[39] V. Mourik, K. Zuo, S. M. Frolov, S. R. Plissard, E. P. A. A. Bakkers, and L. P. Kouwenhoven, Signatures of Majorana fermions in hybrid superconductor-semiconductor nanowire devices, Science **336**, 1003 (2012).
[40] E. J. H. Lee, X. Jiang, R. Aguado, G. Katsaros, C. M. Lieber, and S. De Franceschi, Zero-Bias Anomaly in a Nanowire Quantum Dot Coupled to Superconductors, Phys. Rev. Lett. **109**, 186802 (2012).
[41] A. Das, Y. Ronen, Y. Most, Y. Oreg, M. Heiblum, and H. Shtrikman, Zero-bias peaks and splitting in an Al-InAs nanowire topological superconductor as a signature of Majorana fermions, Nat. Phys. **8**, 887 (2012).
[42] M. T. Deng, C. L. Yu, G. Y. Huang, M. Larsson, P. Caroff, and H. Q. Xu, Anomalous zero-bias conductance peak in a Nb-InSb nanowire-Nb hybrid device, Nano Lett. **12**, 6414 (2012).
[43] W. Chang, V. E. Manucharyan, T. S. Jespersen, J. Nygard, and C. M. Marcus, Tunneling Spectroscopy of Quasiparticle Bound States in a Spinful Josephson Junction, Phys. Rev. Lett. **110**, 217005 (2013).
[44] E. J. H Lee, X. Jiang, M. Houzet, R. Aguado, C. M. Lieber, and S. De Franceschi, Spin-resolved Andreev levels and parity crossings in hybrid superconductor-semiconductor nanostructures, Nat. Nanotechnol. **9**, 79 (2014).
[45] R. Žitko, J. S. Lim, R. Lopez, and R. Aguado, Shiba states and zero-bias anomalies in the hybrid normal-superconductor Anderson model, Phys. Rev. B **91**, 045441 (2015).
[46] N. Wentzell, S. Florens, T. Meng, V. Meden, and S. Andergassen, Magneto-electric spectroscopy of Andreev bound states in Josephson quantum dots, Phys. Rev. B **94**, 085151 (2016).
[47] A. Jellinggaard, K. Grove-Rasmussen, M. H. Madsen, and J. Nygard, Tuning Yu-Shiba-Rusinov states in a quantum dot, Phys. Rev. B **94**, 064520 (2016).
[48] B. Bujnowski, D. Bercioux, F. Konschelle, J. Cayssol, and F. S. Bergeret, Andreev spectrum of a Josephson junction with spin-split superconductors, Europhys. Lett. **115**, 67001 (2016).
[49] A. Y. Kitaev, Unpaired Majorana fermions in quantum wires, Phys.-Usp. **44**, 131 (2001).
[50] S. Nadj-Perge, I. K. Drozdov, B. A. Bernevig, and A. Yazdani, Proposal for realizing Majorana fermions in chains of magnetic atoms on a superconductor, Phys. Rev. B **88**, 020407 (2013).
[51] S. Nadj-Perge, I. K. Drozdov, J. Li, H. Chen, S. Jeon, J. Seo, A. H. MacDonald, B. A. Bernevig, and A. Yazdani, Observation of Majorana fermions in ferromagnetic atomic chains on a superconductor, Science **346**, 602 (2014).
[52] M. Ruby, F. Pientka, Y. Peng, F. von Oppen, B. W. Heinrich, and K. J. Franke, End States and Subgap Structure in Proximity-Coupled Chains of Magnetic Adatoms, Phys. Rev. Lett. **115**, 197204 (2015).
[53] J. D. Sau, R. M. Lutchyn, S. Tewari, and S. Das Sarma, Generic New Platform for Topological Quantum Computation using Semiconductor Heterostructures, Phys. Rev. Lett. **104**, 040502 (2010).
[54] J. Alicea, Y. Oreg, G. Refael, F. van Oppen, and M. P. A. Fischer, Non-Abelian statistics and topological quantum information processing in 1D wire networks, Nat. Phys. **7**, 412 (2011).
[55] S. Das Sarma, M. Freedman, and C. Nayak, Majorana zero modes and topological quantum computation, npj Quantum Inform. **1**, 15001 (2015).
[56] R. Meservey, P. M. Tedorow, and P. Fulde, Magnetic Field Splitting of the Quasiparticle States in Superconducting Aluminum Films, Phys. Rev. Lett. **25**, 1270 (1970).
[57] P. M. Tedrow and R. Meservey, Spin-Dependent Tunneling into Ferromagnetic Nickel, Phys. Rev. Lett. **26**, 192 (1971).
[58] P. M. Tedrow and R. Meservey, Spin polarization of electrons tunneling from films of Fe, Co, Ni, and Gd, Phys. Rev. B **7**, 318 (1973).
[59] R. Meservey and P. M. Tedrow, Spin-polarized electron tunneling, Phys. Rep. **238**, 173 (1994).
[60] M. Eltschka, B. Jäck, M. Assig, O. V. Kondrashov, M. A. Skvortsov, M. Etzkorn, C. R. Ast, and K. Kern, Probing absolute spin polarization at the nanoscale, Nano Lett. **14**, 7171 (2014).
[61] J. Linder and J. W. A. Robinson, Superconducting spintronics, Nat. Phys. **11**, 307 (2015).
[62] C. Csonka, L. L. Hofstetter, F. Freitag, S. Oberholzer, C. Schönberger, T. S. Jespersen, M. Aegesen, and J. Nygard, Giant fluctuations and gate control of the g-factor in InAs nanowire quantum dots, Nano Lett. **8**, 3932 (2008).
[63] T. Nakaoka, T. Saito, J. Tatebayashi, S. Hirose, T. Usuki, N. Yokoyama, and Y. Arakawa, Tuning of g-factor in self-assembled In(Ga)As quantum dots through strain engineering, Phys. Rev. B **71**, 205301 (2005).
[64] J. van Bree, A. Y. Silov, M. L. van Maasakkers, C. E. Pryor, M. E. Flatté, and P. M. Koenraad, Anisotropy of electron and hole gtensors of quantum dots: An intuitive picture based on spin-correlated orbital currents, Phys. Rev. B **93**, 035311 (2016).
[65] M. D. Schroer, K. D. Petersson, M. Jung, and J. R. Petta, Field Tuning the g Factor in Inas Nanowire Double Quantum Dots, Phys. Rev. Lett. **107**, 176811 (2011).
[66] R. S. Deacon, Y. Kanai, S. Takahashi, A. Oiwa, K. Yoshida, K. Shibata, K. Hirakawa, Y. Tokura, and S. Tarucha, Electrically tuned g tensor in an InAs self-assembled quantum dot, Phys. Rev. B **84**, 041302 (2011).

[67] N. Ares, V. N. Golovach, G. Katsaros, M. Stoffel, F. Fournel, L. I. Glazman, O. G. Schmidt, and S. De Franceschi, Nature of Tunable Hole g Factors in Quantum Dots, Phys. Rev. Lett. **110**, 046602 (2013).
[68] K. G. Wilson, The renormalization group: Critical phenomena and the Kondo problem, Rev. Mod. Phys. **47**, 773 (1975).
[69] H. R. Krishna-murthy, J. W. Wilkins, and K. G. Wilson, Renormalization-group approach to the Anderson model of dilute magnetic alloys, I: Static properties for the symmetric case, Phys. Rev. B **21**, 1003 (1980).
[70] W. Hofstetter, Generalized Numerical Renormalization Group for Dynamical Quantities, Phys. Rev. Lett. **85**, 1508 (2000).
[71] R. Žitko and T. Pruschke, Energy resolution and discretization artefacts in the numerical renormalization group, Phys. Rev. B **79**, 085106 (2009).
[72] R. Žitko, Adaptive logarithmic discretization for numerical renormalization group methods, Comput. Phys. Commun. **180**, 1271 (2009).
[73] T. Hecht, A. Weichselbaum, J. von Delft, and R. Bulla, Numerical renormalization group calculation of near-gap peaks in spectral functions of the Anderson model with superconducting leads, J. Phys.: Condens. Matter **20**, 275213 (2008).
[74] R. Bulla, T. Costi, and T. Pruschke, The numerical renormalization group method for quantum impurity systems, Rev. Mod. Phys. **80**, 395 (2008).
[75] M. Höck and J. Schnack, Numerical renormalization group calculations of the magnetization of Kondo impurities with and without uniaxial anisotropy, Phys. Rev. B **87**, 184408 (2013).
[76] R. Žitko, R. Peters, and T. Pruschke, Properties of anisotropic magnetic impurities on surfaces, Phys. Rev. B **78**, 224404 (2008).
[77] A. M. Clogston, Upper Limit for the Critical Field in Hard Superconductors, Phys. Rev. Lett. **9**, 266 (1962).
[78] B. S. Chandrasekhar, A note on the maximum critical field of high-field superconductors, Appl. Phys. Lett. **1**, 7 (1962).
[79] K. Machida and F. Shibata, Bound states due to resonance scattering in superconductor, Prog. Theor. Phys. **47**, 1817 (1972).